The Rho5 GTPase is necessary for oxidant-induced cell death in budding yeast

Komudi Singh, Pil Jung Kang, and Hay-Oak Park*

Department of Molecular Genetics, Ohio State University, Columbus, OH 43210

Edited by Gregory A. Petsko, Brandeis University, Waltham, MA, and approved December 12, 2007 (received for review August 4, 2007)

In both animal and yeast cells, reactive oxygen species (ROS) are produced as byproducts of metabolism and upon exposure to diverse environmental stresses. Cellular defense systems operate to avoid molecular damage caused by ROS, but the redox balance is disturbed under excessive stress. Cells of the budding yeast *Saccharomyces cerevisiae* undergo apoptotic-like cell death upon exposure to hydrogen peroxide (H_2O_2). Here, we report that the Rho5 GTPase of budding yeast is necessary for H_2O_2-induced cell death, which accompanies ROS accumulation and DNA fragmentation. Unlike WT, a *rho5* deletion mutant (*rho5*Δ) exhibits little cell death, whereas the constitutively active *rho5*^{G12V} mutant exhibits excess ROS accumulation and increased cell death upon H_2O_2 treatment. Consistent with a role in the oxidative stress response, Rho5 interacts with the thioredoxin reductase Trr1, a key component of the cytoplasmic thioredoxin antioxidant system, in a GTP-dependent manner. This interaction occurs on the vacuolar membrane before exposure to H_2O_2 but also in the vacuolar lumen after H_2O_2 treatment. Trr1 levels are elevated in *rho5*Δ cells but are elevated only slightly in WT and not in the *rho5*^{G12V} cells after H_2O_2 treatment. Taken together, these data suggest that Rho5 mediates H_2O_2-induced cell death by regulating the level of Trr1 or by excluding Trr1 from its cytoplasmic substrate.

thioredoxin reductase | apoptosis | reactive oxygen species

Changes in the intracellular redox state regulate several critical intracellular pathways in mammalian cells (1). In *Saccharomyces cerevisiae*, as in higher eukaryotes, reactive oxygen species (ROS) are produced as normal byproducts of cellular metabolism. The increased production of ROS triggers defense mechanisms to avoid the deleterious consequence of ROS accumulation. The glutathione (GSH)/glutaredoxin (GRX), and thioredoxin (TRX) systems are major cellular factors that are involved in the regulation of redox homeostasis. Thiol groups (-SH) of these components play a remarkably broad range of roles in the cell, and the redox status of the cysteine residues can affect both the structure and function of numerous proteins (2). In budding yeast, *TRR1* encodes the cytoplasmic thioredoxin reductase that reduces the oxidized disulfide form of TRX by using NADPH and is required for the protection of yeast cells against oxidative and reductive stress (3). Budding yeast also contains a mitochondrial thioredoxin system, which is thought to protect cells against the oxidative stress generated during respiratory metabolism (4).

The redox balance is disturbed when yeast cells are exposed to diverse environmental stresses such as oxidants, heat shock, and metal ions. It has been reported that H_2O_2 treatment triggers apoptotic cell death in yeast as in various mammalian cells (5, 6), although to what extent the cell death program is conserved from yeast to mammals is not clear (for reviews, see refs. 7–9). Small GTPases are involved in both apoptotic and necrotic cell death (10–12) as well as production of ROS in higher eukaryotes (13). In particular, Rac GTPases are involved in activation of NADPH oxidase, which accepts electrons from NADPH to produce the superoxide radical, in neutrophils and nonphagocytic cells (13, 14). However, the signaling pathways involved in the oxidative stress response and maintenance of redox homeostasis are not well established in any cell type. To decipher the role of small GTPases in the signaling and execution pathways of these programs, we have used the genetically tractable budding yeast.

Rho5 in *S. cerevisiae* shares ≈45% sequence identity with Rac GTPases and contains a Ras-like effector region, which is identical to that of Cdc42 (15). Although it has been reported that a deletion of *RHO5* confers resistance to drugs such as caffeine and Calcofluor white (16), its cellular function is not well understood. Given its structural similarity to Rac, we asked whether Rho5 affects redox homeostasis in yeast. Here, we report that Rho5 is necessary for H_2O_2-induced cell death. We also present both *in vitro* and *in vivo* data indicating that Rho5 interacts with Trr1 and affects the Trr1 levels. Our data support the idea that Rho5-GTP contributes to ROS accumulation and ultimately to cell death upon H_2O_2 treatment by lowering Trr1 levels in the cytoplasm.

Results

***A rho5* Deletion Mutant Is Resistant to Oxidants.** To test whether Rho5 affects the redox balance in yeast, we first examined the growth phenotype of *rho5* mutants in the presence of oxidizing agents such as diethylmaleate (DEM), a thiol-specific oxidant that depletes glutathione in the cell, and paraquat, a superoxide-generating agent, both of which increase intracellular ROS levels (17–19). Although both WT and a *rho5*Δ mutant grew at approximately the same rate in the absence of oxidants, *rho5*Δ grew better (≈10-fold) than WT on plates containing DEM or paraquat (Fig. 1*A*). To examine whether the sensitivity to oxidants depends on the guanine nucleotide-bound state of Rho5, we used a constitutively active *rho5* mutant (*rho5*^{G12V}), which carries a substitution of Gly at position 12 with Val. We also generated a dominant-negative *rho5* mutant (*rho5*^{K16N}), which is expected to express the constitutively GDP-bound (or nucleotide-empty) Rho5. The *rho5*Δ cells carrying each mutant or a WT *RHO5* plasmid were tested for their growth on oxidant-containing plates. Although there was a relatively mild difference in sensitivity, the *rho5*Δ cells carrying the *rho5*^{G12V} plasmid were more sensitive to the oxidants than the cells carrying the WT plasmid or vector control, whereas the *rho5*Δ cells carrying the *rho5*^{K16N} plasmid were more resistant to the oxidants than the cells carrying the WT plasmid (Fig. 1*B*). Because H_2O_2 has been shown to trigger apoptotic-like cell death in budding yeast (5, 20), we next examined cell viability of *rho5* mutants after H_2O_2 treatment (see *Materials and Methods* for details). Consistent with previous reports (5), the WT strain

Author contributions: K.S., P.J.K., and H.-O.P. designed research; K.S. and P.J.K. performed research; K.S. and P.J.K. contributed new reagents/analytic tools; K.S., P.J.K., and H.-O.P. analyzed data; and K.S., P.J.K., and H.-O.P. wrote the paper.

The authors declare no conflict of interest.

This article is a PNAS Direct Submission.

*To whom correspondence should be addressed at: Department of Molecular Genetics, Ohio State University, 484 West 12th Avenue, Columbus, OH 43210-1292. E-mail: park.294@osu.edu.

This article contains supporting information online at www.pnas.org/cgi/content/full/0707359105/DC1.

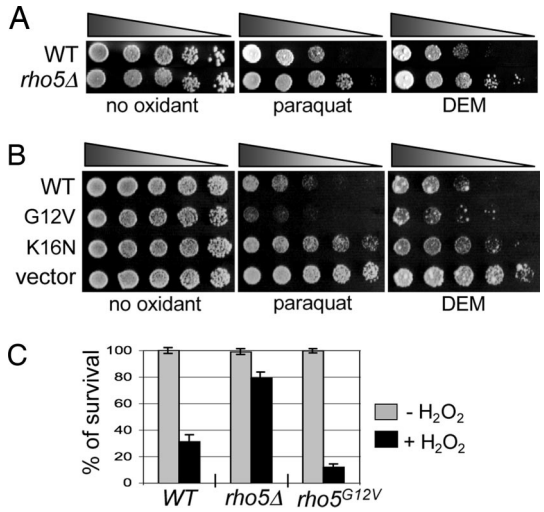

Fig. 1. Phenotype of *rho5* mutants. (*A*) Tenfold serial dilutions of WT (HPY210) and *rho5*Δ mutant (HPY720) cells starting from equal OD_{600} unit were grown at 30°C for 2–5 d on YPD or YPD containing 400 μg/ml of paraquat or 1 mM DEM. The triangles above the images in *A* and *B* represent the decrease of cell numbers plated in each spot. (*B*) A *rho5*Δ mutant (HPY720) carrying 2μ plasmids of *RHO5* (WT), $rho5^{G12V}$ (G12V), or $rho5^{K16N}$ (K16N) or empty vector was plated in 2.5-fold serial dilutions on SC plates lacking uracil and containing 200 μg/ml of paraquat, 1 mM DEM, or no oxidant. Note: Spontaneous suppressors frequently arose on DEM-containing plates. (*C*) Survival of WT, *rho5*Δ, and $rho5^{G12V}$ (HPY999) after 4-h incubation with 4.4 mM H_2O_2 (black bar) or without H_2O_2 (gray bar). Data represent mean ± SD from four independent experiments (n = 550–650 cells of each strain plated for each experiment).

exhibited ≈30% viability after H_2O_2 treatment. Interestingly, the *rho5*Δ mutant exhibited much higher cell survival (≈80%), whereas cells expressing $Rho5^{G12V}$ from the chromosomal locus exhibited less cell survival (≈10%) after H_2O_2 treatment (Fig. 1*C*). Taken together, these results suggest that Rho5-GTP is necessary for oxidant-induced cell death of budding yeast.

Cells Lacking Rho5 Do Not Display Apoptotic Phenotype After H_2O_2 Treatment. To test whether Rho5-dependent cell death associates with apoptotic phenotypes such as ROS accumulation and DNA fragmentation, we first monitored the intracellular ROS level with dihydrorhodamine 123 (DHR), which accumulates in the cell and becomes fluorescent rhodamine 123 upon oxidation (21). Before exposure to H_2O_2, little fluorescence was detectable in WT and *rho5* mutants (see Fig. 2*B*). After H_2O_2 treatment, the fluorescent signal dramatically increased in the $rho5^{G12V}$ cells and to a lesser extent in WT but little in the *rho5*Δ cells (Fig. 2*A*). Analysis of these cells by flow cytometry also indicated a high level of ROS in $rho5^{G12V}$ after H_2O_2 treatment but not in *rho5*Δ, whereas little fluorescence was detected in all these cells before H_2O_2 treatment (Fig. 2*B*).

We next examined nuclei with 4′,6-diamidino-2-phenylindole (DAPI) staining. The *rho5*Δ cells showed intact round nuclei and mitochondrial DNA, which appeared as smaller dots predominantly located near the periphery of the cells, before (data not shown) and after H_2O_2 treatment (Fig. 2*C*). In contrast, ≈62% of the $rho5^{G12V}$ cells showed misshapen or fragmented nuclei, and most of them lacked mitochondrial DNA staining after H_2O_2 treatment (Fig. 2*C*). The $rho5^{G12V}$ mutant, however, was able to grow on the medium based on the nonfermentable carbon source, and showed normal nuclear and mitochondrial DNA staining before H_2O_2 treatment (data not shown), suggesting that the mutant cells contain the functional mitochondria. These cells were also double-stained by terminal deoxynucleotidyl transferase (TdT)-mediated dUTP nick end labeling (TUNEL) to detect DNA fragmentation, which is a hallmark of apoptosis. Although no TUNEL-positive cells were found before H_2O_2 treatment, 87% of $rho5^{G12V}$ and 76% of WT cells were TUNEL-positive after H_2O_2 treatment, whereas 23% of the *rho5*Δ cells were TUNEL-positive (Fig. 2*D*). Taken together, these data suggest that Rho5 is involved in apoptotic cell death induced by H_2O_2.

Localization of Rho5-GFP and $Rho5^{G12V}$-GFP Before and After H_2O_2 Treatment. To gain insight into how Rho5 is involved in H_2O_2-induced cell death, we examined localization of Rho5 using a functional GFP fusion expressed from its chromosomal locus [see supporting information (SI) *Methods*]. We also examined $Rho5^{G12V}$-GFP localization using a strain that is similar except for the $rho5^{G12V}$ mutation. Before exposure to H_2O_2, both Rho5-GFP and $Rho5^{G12V}$-GFP localized to the plasma membrane and to the endomembranes, mainly the vacuolar membrane based on staining with the vital dye FM4–64 (Fig. 3 *A* and *B a–c*), which is delivered to the vacuolar membrane via an endocytic transport route (22). After H_2O_2 treatment, Rho5-GFP also appeared in the vacuolar lumen in addition to the membranes (25 ≈ 60%) (Fig. 3*A d–f*), whereas $Rho5^{G12V}$-GFP appeared in a punctate pattern (35≈65%) but little on the plasma membrane. Most patches of $Rho5^{G12V}$-GFP overlapped with the patches from FM4–64 staining (Fig. 3*B d–f*), suggesting that $Rho5^{G12V}$-GFP localized to the endocytic (and/or secretory) vesicles.

Rho5 Interacts with Trr1 in a GTP-Dependent Manner. To understand how Rho5 is involved in H_2O_2-induced cell death, we attempted to identify proteins that interact with Rho5. We focused on Trr1 because it copurified with Rho5 in a high-throughput interaction study (23) and because it is a key component in the thioredoxin antioxidant system, which activates thioredoxin peroxidase and is known to inhibit apoptosis (24). To determine whether Rho5 indeed interacts with Trr1, and, if so, whether the interaction depends on the GTP-bound state of Rho5, we took three different approaches. First, an *in vitro* binding assay was carried out by using Rho5 purified as a fusion to GST. GST-Rho5, preloaded with GTPγS or GDP or in the nucleotide-empty state, was incubated with yeast extract carrying the Myc epitope-tagged Trr1. When GST-Rho5 was pulled down with glutathione Sepharose beads from the reaction mixtures, Trr1 coprecipitated with Rho5-GTPγS, but much less efficiently with Rho5-GDP, nucleotide-empty state of Rho5 or GST control (Fig. 4*A*), suggesting that Trr1 associates preferentially with Rho5-GTP *in vitro*.

Second, we carried out a yeast two-hybrid assay using the *LEU2* reporter and plasmids expressing Trr1 fused to the acidic activation domain and Rho5 fused to the DNA-binding domain (25). Cells expressing $Rho5^{G12V}$ (and Rho5 to a lesser extent) grew on the plate lacking Leu, whereas cells expressing $Rho5^{K16N}$ or carrying vector controls grew poorly (Fig. 4*Bb*), suggesting that Trr1 interacts with Rho5-GTP *in vivo*. When these cells were tested on the DEM-containing (and lacking Leu) plates, cells expressing Rho5 grew almost equally to cells expressing $Rho5^{G12V}$ (Fig. 4*Bc*), suggesting that more Rho5 is activated in the presence of DEM.

Finally, we used a bimolecular fluorescence complementation assay (BiFC) (26) to monitor whether and where Rho5 interacted with Trr1 in live cells. Trr1 was expressed as a fusion to the N-terminal half of the yellow fluorescent protein (YFP^N), whereas WT and mutant Rho5 proteins were expressed as fusions to the C-terminal half of YFP (YFP^C). Although each truncated YFP fragment was nonfluorescent (data not shown), *in vivo* interaction between Rho5 and Trr1 brought these two fragments together, and they then produced a fluorescent signal.

CELL BIOLOGY

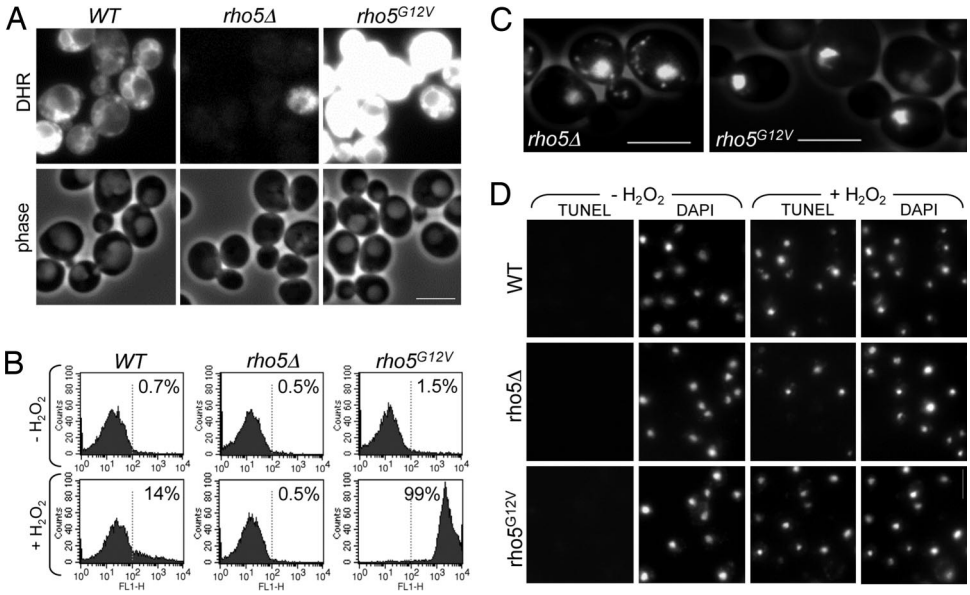

Fig. 2. Apoptotic phenotype of WT and *rho5*^{G12V} after H_2O_2 treatment. (*A*) Cells of WT, *rho5*Δ, and *rho5*^{G12V} were visualized by fluorescence microscopy after staining with DHR during H_2O_2 treatment. Before H_2O_2 treatment and during the first 1-h incubation with H_2O_2, little ROS was detected in all strains, but it became significantly different among the strains after 2-h incubation with H_2O_2. Fluorescence (*Upper*) and phase (*Lower*) images of representative cells after 4-h H_2O_2 treatment are shown. (n ≈ 250 cells for each sample in four independent experiments). (Scale bar: 5 μm.) (*B*) FACS analysis of cells after the same treatment with DHR as in *A* with (+H_2O_2) or without (−H_2O_2) H_2O_2 treatment. Histograms of single representative experiment are shown from three independent experiments. *n* = 10,000 per sample. (*C*) DAPI staining of the *rho5*Δ and *rho5*^{G12V} mutants after H_2O_2 treatment. Approximately 62% of the *rho5*^{G12V} cells showed misshapen or fragmented nuclei, and >95% of the cells were lacking mitochondrial DNA staining (*n* = 400), whereas >90% of the *rho5*Δ cells showed normal nuclear and mitochondrial DNA (*n* = 200). Phase-contrast images with dim light were merged with fluorescence images to show cell boundaries. Small dots appearing near the periphery of the *rho5*Δ cells represent mitochondrial DNA. (Scale bars: 5 μm.) (*D*) TUNEL staining of WT, *rho5*Δ, and *rho5*^{G12V} cells before (−H_2O_2) and after (+H_2O_2) incubation with H_2O_2. DAPI staining of the same cells is also shown. The percentage (mean ± SD) of TUNEL-positive cells after H_2O_2 treatment from three independent experiments: WT, 76.3 ± 3.8 (*n* = 325); *rho5*^{G12V}, 87.3 ± 3.2 (*n* = 350); *rho5*Δ, 23.4 ± 5.9 (*n* = 350). Less than 1% of cells were TUNEL-positive in all strains before H_2O_2 treatment. (Scale bars: 5 μm.)

Before exposure to H_2O_2, Rho5-YFP^C and Rho5^{G12V}-YFP^C, in combination with Trr1-YFP^N, exhibited the YFP signal on the vacuolar membrane, whereas little YFP signal was detected with Rho5^{K16N}-YFP^C before and after H_2O_2 treatment (Fig. 4*C a–c* and *f*), suggesting that Rho5-GTP interacted with Trr1 on the vacuolar membrane. The absence of the fluorescent signal in cells expressing Rho5^{K16N}-YFP^C and Trr1-YFP^N is unlikely to be due to low levels of expression or instability of the mutant protein, because all YFP^C fusions were present at approximately equal levels (SI Fig. 6). After H_2O_2 treatment, Rho5-YFP^C and Trr1-YFP^N colocalized to the lumen or the membrane of the vacuole and also often in a patch, which appeared on the vacuolar membrane (Fig. 4*Cd*), whereas Rho5^{G12V}-YFC^C and Trr1-YFP^N colocalized in a punctate pattern in the cytoplasm (Fig. 4*Ce*). This localization pattern was similar to that of Rho5^{G12V}-GFP, suggesting that these patches are likely in the endocytic (and/or secretory) vesicles. Taken together, these data suggest that Rho5-GTP interacts with Trr1 and the interaction occurs at distinct subcellular compartments.

Rho5-GTP May Inhibit the Elevation of Trr1 Level upon H_2O_2 Treatment. Trr1 is known as a cytoplasmic protein (27–29), and its level is induced under mild oxidative stress (for example, upon exposure to 0.3–1 mM H_2O_2) (30, 31). We wished to know whether Trr1 was also elevated under the condition that induced apoptotic cell death and whether Trr1 localization changed after H_2O_2 treatment in a Rho5-dependent manner. We expressed Trr1 as a fusion to mCherry, a red fluorescent protein (32), from its chromosomal locus and observed its localization over time after addition of H_2O_2 (4.4 mM). Although the Trr1-mCherry fluorescence signal appeared throughout the cytoplasm before and after H_2O_2 treatment in WT and *rho5* mutants (Fig. 5*A*; data not shown), the fluorescence intensity was different in these strains, in particular upon H_2O_2 treatment. The fluorescence intensities of >100 cells of each strain were analyzed by the line intensity plot (see SI Fig. 7). The Trr1-mCherry fluorescence increased ≈2-fold in the *rho5*Δ cells at 4 h after H_2O_2 treatment (Fig. 5*A*). However, there was almost no increase of the fluorescence in the *rho5*^{G12V} cells and very little increase in WT (unlike the case of mild oxidative stress) (Fig. 5*A*), whereas a control Vph1-GFP fluorescence remained approximately the same in each strain. These cells were also analyzed by flow cytometry. Consistent with the microscopic observation, the number of cells with higher fluorescence was increased in the *rho5*Δ mutant, but not in the *rho5*^{G12V} mutant, after exposure to H_2O_2 [Fig. 5*B*; compare the thick black line (+H_2O_2) to the thin line with filled area below (−H_2O_2)].

Next, we compared the Trr1 protein level using the HA epitope-tagged Trr1. Consistent with the Trr1-mCherry fluorescence, the Trr1-HA level was most elevated in *rho5*Δ, but not in the *rho5*^{G12V} mutant, after H_2O_2 treatment. Trr1 levels appeared lower in *rho5*^{G12V} compared with WT even before exposure to H_2O_2 (based on both Trr1-mCherry fluorescence and protein blot). Taken together, these data suggest that the cytoplasmic Trr1 level is elevated in the *rho5*Δ cells, which exhibit little cell death after H_2O_2 treatment, but not in the *rho5*^{G12V} cells, which undergo apoptotic cell death. Because lower Trr1 level is likely to result in lower thioredoxin peroxidase activity, which reduces H_2O_2 (27), we asked whether overexpression of *TSA1*, which encodes a cytoplasmic thioredoxin peroxidase, suppresses apoptotic cell death of WT or the *rho5*^{G12V} mutant. The WT cells carrying the multicopy *TSA1* plasmid exhibited higher cell viability (≈47%) after H_2O_2 treatment compared with the vector control (≈36%), suggesting that

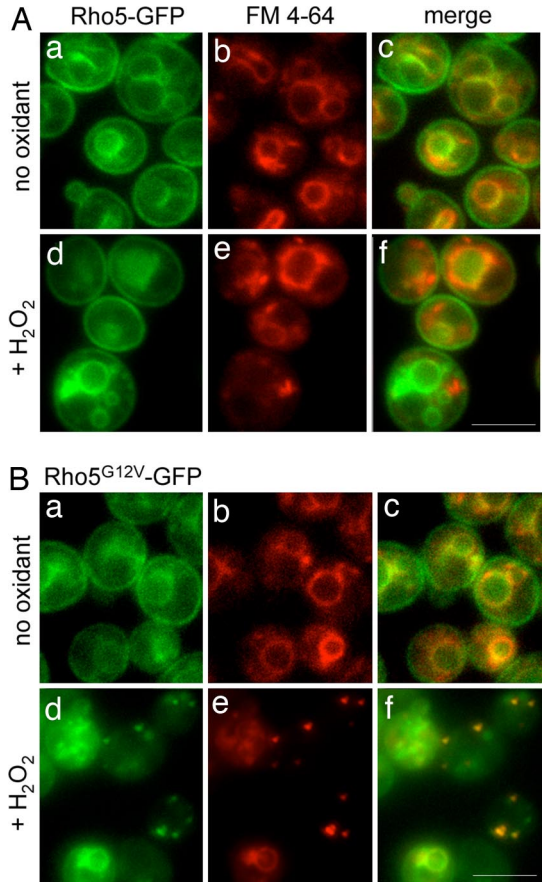

Fig. 3. Localization of Rho5-GFP (*A*) and Rho5^{G12V}-GFP (*B*) before and after H_2O_2 treatment. GFP fusions of WT (HPY1156) and Rho5^{G12V} (HPY1157) were expressed from the chromosomal *RHO5* locus. Rho5-GFP was functional based on sensitivity of HPY1156 to oxidants. Staining with FM4–64 was done for 40 min. Series of Z-section images were projected into two-dimensional images. (Scale bars: 5 μm.)

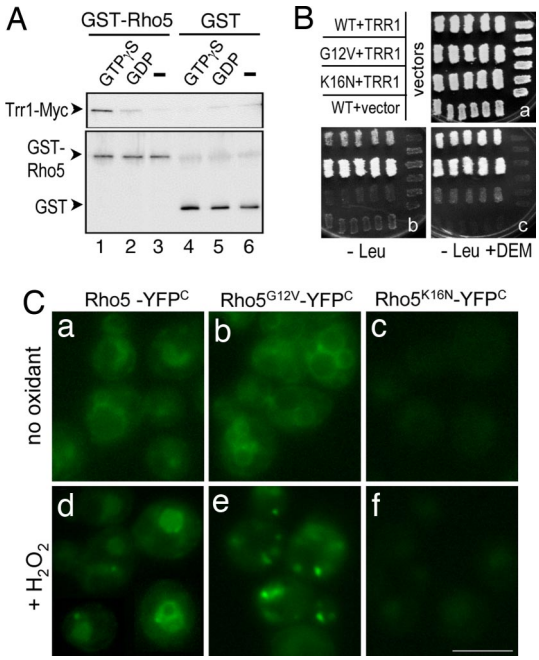

Fig. 4. Interaction between Rho5 and Trr1. (*A*) GST-Rho5 preloaded with GTPγS (lane 1) or GDP (lane 2) or after nucleotide-depletion (lane 3) was incubated with yeast extract carrying Trr1-Myc. GST was treated similarly (lanes 4–6). GST-Rho5 and GST were pulled down with glutathione Sepharose, and eluent from the beads was detected by immunoblotting after SDS/PAGE. Trr1-Myc was detected with a monoclonal antibody against Myc epitope *(Upper)*; GST-Rho5 and GST were detected with polyclonal antibodies against GST (*Lower*). (*B*) Two-hybrid interaction. Independent transformants of the *TRR1* and *RHO5* (WT), *rho5^{G12V}* (G12V), *rho5^{K16N}* (K16N) plasmids (or vector control) were patched on SC plates lacking Trp and His (*a*) to maintain the plasmids, as depicted at the top left. This plate was then replica-plated onto SGal-Leu, Trp, His (*b*) to monitor expression of the *LEU2* reporter gene and SGal-Leu, Trp, His plus 1 mM DEM (*c*) to monitor *LEU2* expression in the presence of oxidant. (*C*) BiFC between Trr1-YFP^N and YFP^C fusions of Rho5 (HPY1163), Rho5^{G12V} (HPY1164), or Rho5^{K16N} (HPY1165). Trr1-YFP^N and each Rho5-YFP^C fusion were expressed from their chromosomal loci. Approximately 300 cells of each strain were examined before and after H_2O_2 treatment, and representative images are shown. (Scale bar: 5 μm.)

overexpression of *TSA1* can partially suppress H_2O_2-induced cell death (Fig. 5*D*). However, the *rho5^{G12V}* mutant carrying the same plasmid exhibited little increase of cell viability, suggesting that Tsa1 is not active in cells expressing the GTP-locked Rho5.

Discussion

Oxidant-induced cell death has been reported in various cell types including mammalian cells, plants, and yeast (5, 6, 10). Although small GTPases have been implicated in apoptosis (10, 33) and ROS production (34, 35), the mechanisms underlying such cellular responses are poorly understood. Here, we uncover a previously undescribed role of the Rho5 GTPase in H_2O_2-induced cell death in budding yeast. Rho5 is likely to play a major role in transmitting the upstream signal from H_2O_2 to execute cell death, because cells lacking Rho5 exhibit little cell death after H_2O_2 treatment. Rho5-mediated cell death is accompanied by the characteristics of apoptosis such as DNA fragmentation and ROS accumulation. Although the details of the mechanism remain to be established, our study provides a linkage between a Rho GTPase and an antioxidant system to regulate cellular response to oxidative stress. By analogy with DNA damage-induced apoptosis (36), we propose that Rho5-GTP promotes apoptosis of the cells with excess oxidative damage.

Despite its sequence similarity to Rac GTPases in mammals, Rho5 is likely to regulate ROS accumulation in a distinct way. Rac triggers ROS production by activating NADPH oxidases in various cell types (10, 34). Although no gene in *S. cerevisiae* has been directly annotated as NADPH oxidase, we show that Rho5 interacts with Trr1 in a GTP-dependent manner and that the level of Trr1 is not elevated in cells expressing Rho5-GTP after H_2O_2 treatment. Trr1 activates TRXs, which in turn activates thioredoxin peroxidase, thus detoxifying H_2O_2 and other ROS (27). Because Rho5 is necessary for ROS accumulation and cell death after H_2O_2 treatment (this work), Rho5 and Trr1 may function in an antagonistic manner under oxidative stress. Given that most, if not all, downstream targets of GTPases specifically interact with the GTP-bound state of GTPases, we favor the idea that Trr1 is a downstream target of Rho5. Rho5-GTP may inhibit the Trr1's function. Although recombinant Rho5 did not affect Trr1 activity *in vitro* (S. W. Kang, personal communication), we found that the Trr1 protein level was elevated in the *rho5*Δ mutant after H_2O_2 treatment but not in the *rho5^{G12V}* mutant, which is expected to express the constitutively GTP-bound Rho5. Low cytoplasmic Trr1 levels in the *rho5^{G12V}* cells may result in low thioredoxin peroxidase activity and thus promote excess ROS accumulation and subsequent cell death. Although the increase of the Trr1 level in the *rho5*Δ mutant after H_2O_2 treatment does not appear to be substantial, it might be critical for how efficiently cells can detoxify H_2O_2, particularly when cells are exposed to exogenous H_2O_2. Although H_2O_2 is a relatively mild oxidant, it can trigger high accumulation of ROS

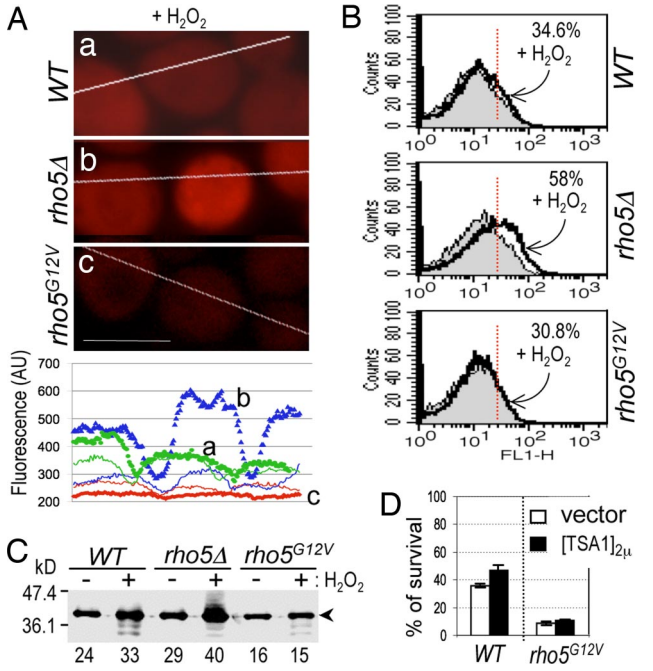

Fig. 5. Elevation of Trr1 in *rho5*Δ after H_2O_2 treatment. (*A*) Localization of Trr1-mCherry in WT and *rho5* mutants after H_2O_2 treatment for 4 h. The fluorescence intensity of the cells along the crossed line is plotted below the images: WT (*a*; green), *rho5*Δ (*b*; blue), and $rho5^{G12V}$ (*c*; red). The fluorescence intensity of the cells before H_2O_2 treatment is shown with the thin line of each color (without showing images). The fluorescence intensities of 25 ≈ 100 cells of each strain before and after 4-h H_2O_2 treatment were analyzed similarly, and they changed as follows (mean ± SD, in arbitrary units): WT from 300 ± 21 ($-H_2O_2$) to 368 ± 51 ($+H_2O_2$), *rho5*Δ from 322 ± 41 ($-H_2O_2$) to 574 ± 122 ($+H_2O_2$), and $rho5^{G12V}$ from 290 ± 18 ($-H_2O_2$) to 265 ± 25 ($+H_2O_2$), whereas a control Vph1-GFP fluorescence remained approximately the same (300 ± 25) in each strain. See SI Fig. 7 for additional line intensity plots of cells at different time points after H_2O_2 addition. (Scale bar: 5 μm.) (*B*) FACS analysis of WT (HPY1160), *rho5*Δ (HPY1159), and $rho5^{G12V}$ (HPY1161) expressing Trr1-mCherry after incubation with H_2O_2 (thick line) or without H_2O_2 (thin line with shaded area). The percentages of the H_2O_2-treated cells with fluorescence higher than the dotted line are given. $n = 10{,}000$. (*C*) Trr1-HA levels in WT and *rho5* mutants. Yeast extracts were prepared from the equal OD_{600} units of the untreated (−) or H_2O_2-treated (+) WT, *rho5*Δ, and $rho5^{G12V}$ cells carrying pRS314-Trr1-HA. Trr1-HA was detected by immunoblotting using a monoclonal HA antibody. Numbers below the panel indicate relative intensity of the Trr1 band (arrowhead) analyzed by using the Odyssey Infrared Imaging System. (*D*) Survival of WT (HPY210) and $rho5^{G12V}$ (HPY999) cells carrying a multicopy *TSA1* plasmid (black bar) or vector control (white bar) after 4-h incubation with 4.4 mM H_2O_2. Data represent mean ± SD from four independent experiments (n = 450–600 cells of each strain plated for each experiment).

by iron-catalyzed reactions (called Fenton reactions) (37). Consistent with this idea, we found that overexpression of *TSA1* partially suppresses the cell death of WT upon exposure to H_2O_2. However, overexpression of *TSA1* does not suppress H_2O_2-induced cell death of the $rho5^{G12V}$ cells, suggesting that Tsa1 may not be activated in cells expressing GTP-locked Rho5 despite its overexpression. However, these genetic data provide only indirect evidence, and alternative interpretations are also possible. Further molecular analyses would be necessary to understand the mechanism by which Rho5 regulates the TRX system.

How might Rho5 regulate the Trr1 level? It is possible that Rho5-GTP inhibits the expression of *TRR1* or promotes degradation of Trr1. Given the physical interaction between Rho5-GTP and Trr1 (this study), we favor the idea that Rho5-GTP is directly involved in regulating Trr1 function. Our BiFC data suggest that a fraction of Trr1 specifically interacts with Rho5 on the vacuolar membrane before exposure to H_2O_2 but also in the vacuolar lumen after H_2O_2 treatment. This translocation of Trr1 into the vacuolar lumen may contribute to the lower Trr1 levels in the cytoplasm. Rho5-GTP may thus be involved in targeting Trr1 to the vacuole to promote its degradation or to exclude Trr1 from its substrate. Surprisingly, $Rho5^{G12V}$ interacts with Trr1 in several patches in the cytoplasm after H_2O_2 treatment. Similarly, $Rho5^{G12V}$-GFP localized to several patches in the cytoplasm, most of which overlap with the FM4–64 staining pattern, suggesting that these patches colocalize to the endosomes. Although we do not have a clear explanation for this observation, it is possible that these patches reflect intermediate localization patterns in the process of targeting Trr1 to the vacuole. In fact, we observed that endocytosis significantly slows down in the $rho5^{G12V}$ mutant after H_2O_2 treatment (see FM4–64 staining in Fig. 3*B*; K.S. and H.-O.P., unpublished observation).

Although recombinant Rho5 did not inhibit Trr1 activity, we also cannot rule out the possibility that Rho5-GTP undergoes additional modification *in vivo*, which might be required for its function to inhibit Trr1. Our two-hybrid data indicate that Rho5–Trr1 interaction increases on the DEM-containing plate, suggesting that more Rho5 is converted to the GTP-bound state in the presence of oxidants. On the other hand, the $rho5^{G12V}$ mutant does not exhibit lethality before H_2O_2 treatment, supporting the idea that Rho5-GTP may be further activated upon exposure to H_2O_2, perhaps through a posttranslational modification or interaction with another protein. Whether Rho5 has additional targets to regulate cell death is not known. It is interesting to note that OsRac1, a Rac GTPase in rice, has been implicated in activation of NADPH oxidase and also in inhibition of expression of the ROS scavenger metallothionein during defense signaling in rice (38). Similarly to OsRac1, Rho5 might negatively regulate another ROS scavenger (such as Trx) through Trr1 and also activate an inducer of ROS production. It is yet to be determined whether such an inducer is present in budding yeast.

Several recent reports suggest that yeast cells undergo "programmed cell death" in response to oxidants and acetic acids, and also during mating and aging, but whether all these cases are apoptotic (as a caspase-mediated death) or nonapoptotic cell death is not clear (8, 9). Whether the Rho5-mediated cell death program involves other proteins such as Yca1 (metacaspase) (39, 40) and Aif1 (apoptosis-inducing factor) (41) remains to be determined. Although mechanistic details are likely to be different among the various species, studies in yeast are expected to provide a better understanding of the multiple cell death programs.

Materials and Methods

Details of cloning, strain construction, and additional methods are provided in *SI Methods*.

Growth Phenotype and Cell Viability Assay. WT and *rho5*Δ strains were diluted to OD_{600} = 0.4 from a mid- to late-logarithmic phase culture in YPD and then serially diluted (10-fold). These cells were spotted on YPD plates containing 400 μg/ml paraquat (Sigma–Aldrich), 1 mM diethyl maleate (Sigma–Aldrich), or no oxidant. The *rho5*Δ strain carrying each *RHO5* plasmid was tested similarly but in 2.5-fold serial dilutions by using SC medium (or plates) lacking uracil and 200 μg/ml paraquat. The plates were incubated at 30°C for 2–7 days. To test cell viability, cells were diluted to OD_{600} = 0.4 from the exponentially growing cultures. A portion of the diluted cells was grown in the presence of 4.4 mM H_2O_2 for 4 h or mock-treated. The number of viable cells was estimated by counting colonies formed from equal OD_{600} units of each culture plated before and after 4-h incubation with H_2O_2 (or without H_2O_2). Cell viability is given by the ratio (number of viable cells after 4-h incubation/number of viable cells before H_2O_2 treatment) × 100. We also estimated total cell number by directly counting cells with a hemocytometer before plating, and found

similar cell viability. The laboratory WT strains exhibited varying degrees of sensitivity to H_2O_2 depending on the background (see *SI Methods*).

Determination of ROS Accumulation. Cells from the mid-log phase culture were diluted to OD_{600} = 0.3 and then incubated with H_2O_2 (4.4 mM final) for 4 h. This same condition has been used for H_2O_2 treatment throughout the article. For the last 2 h of the incubation with H_2O_2, dihydrorhodamine 123 (Sigma) was added to a final concentration of 5 μg/ml, and then cells were observed under the fluorescence microscope with TRITC filter or subject to flow cytometry by using a FACS Calibur (Becton Dickinson) following the procedure of Madeo *et al.* (5).

Staining and Microscopy. Staining with FM4–64 (Invitrogen) was performed for 40 min as described by Vida and Emr (22). To visualize the nuclei, cells were stained with DAPI (10 μg/ml final) for 5–8 min after H_2O_2 treatment. Localization of GFP and mCherry fusion proteins was determined as described (42) except that, where indicated, cells were treated with H_2O_2 before they were observed under the microscope. Image acquisition was carried out by using a Nikon E800 microscope fitted with a ×100 oil-immersion objective (N.A. = 1.30) as described in ref. 42, except that Slidebook 4 digital microscopy software (Intelligent Imaging Innovations) was used to capture a series of optical sections at 0.3-μm intervals and subsequent image processing and analysis.

Bimolecular Fluorescence Complementation (BiFC). Construction of strains used for BiFC is described in *SI Methods*. The YFP signal was detected as described above except that a single optical section was captured by using the YFP filter and by exposing cells to UV for 10 s. Expression of the YFP^C-fusion proteins was detected by immunoblotting using full-length A.v. GFP polyclonal antibody (Clontech) (SI Fig. 6).

ACKNOWLEDGMENTS. We are grateful to K. W. Cunningham and S. W. Kang for their suggestions; B. Andrews (University of Toronto, Toronto, ON, Canada), H. Madhani (University of California, San Francisco), B. Oakley (Ohio State University, Columbus, OH), D. Bisaro (Ohio State University), R. Piper (University of Iowa, Iowa City, IA), D. Eide (University of Wisconsin, Madison), and F. Doignon (Institut de Biochimie et Génétique Cellulaires, UMR Université Victor Segalen Bordeux 2-CNRS, France; and A. Hopper, B. Oakley, A. Simcox, and E. Oakley for comments on the manuscript. This work was supported by grants from the National Institutes of Health (GM76375), the American Cancer Society-Ohio, and the American Heart Association.

1. Kamata H, Hirata H (1999) *Cell Signal* 11:1–14.
2. Trotter EW, Grant CM (2003) *EMBO J* 4:184–188.
3. Trotter EW, Grant CM (2002) *Mol Microbiol* 46:869–878.
4. Pedrajas JR, Miranda-Vizuete A, Javanmardy N, Gustafsson JA, Spyrou G (2000) *J Biol Chem* 275:16296–16301.
5. Madeo F, Frohlich E, Ligr M, Grey M, Sigrist SJ, Wolf DH, Frohlich K-U (1999) *J Cell Biol* 145:757–767.
6. Cai H (2005) *Cardiovasc Res* 68:26–36.
7. Jin C, Reed JC (2002) *Nat Rev* 3:453–459.
8. Hardwick JM, Cheng WC (2004) *Dev Cell* 7:630–632.
9. Buttner S, Eisenberg T, Herker E, Carmona-Gutierrez D, Kroemer G, Madeo F (2006) *J Cell Biol* 175:521–525.
10. Kawasaki T, Henmi K, Ono E, Hatakeyama S, Iwano M, Satoh H, Shimamoto K (1999) *Proc Natl Acad Sci USA* 96:10922–10926.
11. Lacal JC (1997) *FEBS Lett* 410:73–77.
12. Vanden Berghe T, Declercq W, Vandenabeele P (2007) *Mol Cell* 769–771.
13. Werner E (2004) *J Cell Sci* 117:143–153.
14. Hordijk PL (2006) *Circ Res* 98:453–462.
15. Garcia-Ranea JA, Valencia A (1998) *FEBS Lett* 434:219–225.
16. Schmitz HP, Huppert S, Lorberg A, Heinisch JJ (2002) *J Cell Sci* 115:3139–3148.
17. Carmel-Harel O, Stearman R, Gasch AP, Botstein D, Brown PO, Storz G (2001) *Mol Microbiol* 39:595–605.
18. Alic N, Higgins VJ, Dawes IW (2001) *Mol Biol Cell* 12:1801–1810.
19. Wanke V, Accorsi K, Porro D, Esposito F, Russo T, Vanoni M (1999) *Mol Microbiol* 32:753–764.
20. Ahn S-H, Cheung WL, Hsu JY, Diaz RL, Smith MM, Allis CD (2005) *Cell* 120:25–36.
21. Herker E, Jungwirth H, Lehmann KA, Maldener C, Frohlich K-U, Wissing S, Buttner S, Fehr M, Sigrist S, Madeo F (2004) *J Cell Biol* 164:501–507.
22. Vida TA, Emr SD (1995) *J Cell Biol* 128:779–792.
23. Ho Y, Gruhler A, Heilbut A, Bader GD, Moore L, Adams S-L, Millar A, Taylor P, Bennett K, Boutilier K, *et al.* (2002) *Nature* 415:180–183.
24. Kern JC, Kehrer JP (2005) *Front Biosci* 10:1727–1738.
25. Gyuris J, Golemis E, Chertkov H, Brent R (1993) *Cell* 75:791–803.
26. Hu CD, Chinenov Y, Kerppola TK (2002) *Mol Cell* 9:789–798.
27. Chae HZ, Chung SJ, Rhee SG (1994) *J Biol Chem* 269:27670–27678.
28. Pedrajas JR, Kosmidou E, Miranda-Vizuete A, Gustafsson J-A, Wright APH, Spyrou G (1999) *J Biol Chem* 274:6366–6373.
29. Trotter EW, Grant CM (2005) *Eukaryotic Cell* 4:392–400.
30. Morgan BA, Banks GR, Toone WM, Raitt D, Kuge S, Johnston LH (1997) *EMBO J* 16:1035–1044.
31. Gasch AP, Spellman PT, Kao CM, Carmel-Harel O, Eisen MB, Storz G, Botstein D, Brown PO (2000) *Mol Biol Cell* 11:4241–4257.
32. Shu X, Shaner NC, Yarbrough CA, Tsien RY, Remington SJ (2006) *Biochemistry* 45:9639–9647.
33. Bivona TG, Quatela SE, Bodemann BO, Ahearn IM, Soskis MJ, Mor A, Miura J, Wiener HH, Wright L, Saba SG, *et al.* (2006) *Mol Cell* 21:481–493.
34. Diekmann D, Abo A, Johnston C, Segal AW, Hall A (1994) *Science* 265:531–533.
35. Yang Z (2002) *Plant Cell* 14:S375–388.
36. Norbury CJ, Zhivotovsky B (2004) *Oncogene* 23:2797–2808.
37. Veal EA, Day AM, Morgan BA (2007) *Mol Cell* 26:1–14.
38. Wong HL, Sakamoto T, Kawasaki T, Umemura K, Shimamoto K (2004) *Plant Physiol* 135:1447–1456.
39. Madeo F, Herker E, Maldener C, Wissing S, Lachelt S, Herlan M, Fehr M, Lauber K, Sigrist SJ, Wesselborg S, *et al.* (2002) *Mol Cell* 9:911–917.
40. Khan MAS, Chock PB, Stadtman ER (2005) *Proc Natl Acad Sci USA* 102:17326–17331.
41. Wissing S, Ludovico P, Herker E, Buttner S, Engelhardt SM, Decker T, Link A, Proksch A, Rodrigues F, Corte-Real M, *et al.* (2004) *J Cell Biol* 166:969–974.
42. Kang PJ, Sanson A, Lee B, Park H-O (2001) *Science* 292:1376–1378.